A Consensus-Based Distributed Secondary Control Optimization Strategy for Hybrid Microgrids

Enrique Espina, *Graduate Student Member, IEEE,* Roberto Cárdenas-Dobson, *Senior Member, IEEE,* John W. Simpson-Porco, *Member, IEEE,* Mehrdad Kazerani, *Senior Member, IEEE,* and Doris Sáez, *Senior Member, IEEE*

***Abstract*—In this paper, a new consensus-based distributed secondary control (DSC) strategy is proposed for frequency control, *dc*-voltage regulation, and optimal dispatch (OD) in isolated hybrid *ac/dc*-microgrids (HMGs), while all the units are maintained within limits. The proposed control scheme dispatches the distributed generators (DGs) within the microgrid in compliance with the Karush-Kuhn-Tucker (KKT) conditions of a linear optimal power flow (OPF) formulation. Furthermore, the power through the interlinking converters (*ICs*) is also dispatched to help minimize the total operation cost of the microgrid. The controllers rely on local measurements and information from neighbouring devices at both sides of the microgrid (DGs and *ICs*). Thus, unlike the conventional methods, the microgrid is considered as a single entity and not as three independent systems interacting with one another, and the OD is calculated considering both the *ac*-DGs and *dc*-DGs. Extensive simulations demonstrate a good performance of the controller amid load step changes and unit congestion, driving the system to an optimal economic operation.**

***Index Terms*—Distributed control, hybrid ac/dc microgrid, secondary control, optimization, cost minimization.**

I. Introduction

THE ongoing improvements in power electronic technologies and advances in capabilities of microprocessors, towards implementation of more complex control strategies, have allowed researchers to intensify their efforts in research and development in the area of microgrids (MGs). In the literature, a MG has been defined as an electrical system capable of integrating different distributed generation (DG) units and loads, which can use alternating current (*ac*) or direct current (*dc*), or both [1]–[3]. Considering the advantages of MGs [4], [5], a lot of effort has been devoted to developing control strategies for both *ac* and *dc*-MGs [5]–[7]. Recently, special attention has been given to the study of hybrid *ac/dc*-MGs (HMGs), as HMGs allow for simplified and efficient integration of both *ac* and *dc* generations and loads, as well as energy storage systems into one electrical system [8]. Typically, a HMG is composed by an *ac*-MG and a *dc*-MG, which are interconnected through interlinking converters (*ICs*), as depicted in Fig. 1. This configuration allows for fewer *ac/dc* conversions [9], [10], leading to power quality improvement and power loss reduction.

Controlling the DGs working collaboratively in a HMG is more complex than when the MGs are operating separately. In addition to controlling the local voltages and the power generated by the DGs within each MG, the interaction of the DGs on both sides (i.e., *ac*-DGs and *dc*-DGs) must be controlled.

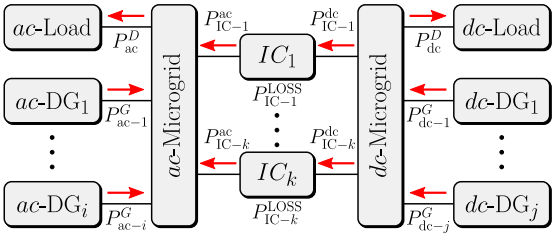

Fig. 1. General topology for a hybrid *ac/dc*-MG with multiple *ICs*.

Thus, control of power transfer through *ICs* is crucial for achieving the required performance of the HMG [11]. On the other hand, the implementation of centralized controllers is not recommended when the MG has a large number of DGs and/or *ICs* since its implementation is infeasible (the computational burden is too high) and it is prone to single-point failures [12], [13]. Therefore, the distributed control approach is preferred since each agent in the MG needs to communicate only with its neighbouring agents, which improves the reliability and security of the MG's operation.

Different objectives can be defined for the operation of the DGs, the most common being active power-sharing among DGs on both sides based on power ratings of units [14], [15], or active power-sharing within MGs and transferring power through the *IC* in case one MG is overloaded [16]. However, in all cases the HMG is considered as three independent systems interacting with one another and not as a single entity. The main focus of this work is on developing a distributed secondary control (DSC) strategy that considers the HMG as a single entity, and not as three independent systems interacting with one another. In addition to restoring the variables modified by the primary control to their nominal values, the proposed control strategy must be capable of solving the optimal dispatch (OD) problem of a HMG in real time, in order to minimize the total operating costs of the MG.

During the last couple of years, significant efforts have been made in the research on HMGs. Consensus-based schemes to minimize the operation cost in HMGs have been reported in [17]–[22]. The authors in [17]–[19] solve the economic dispatch problem in the hybrid *ac/dc*-microgrid with a distributed approach. However, none of these control schemes consider the restoration of the variables modified by the primary control loop. Secondary control has been considered in [20], [21] and a stability analysis has been included in [22]. However, the losses in the *ICs* are not considered in the problem

formulation of these proposals, which is not consistent with one of the objectives of studying hybrid *ac/dc*-microgrids: reducing the *ac*-to-*dc* (and *dc*-to-*ac*) conversion power losses. In conclusion, there is still room for research on this topic since all proposed control strategies have drawbacks and they do not consider a secondary distributed control approach to integrate the secondary variables restoration of both sides in a HMG as a single entity while reducing conversion losses.

The contributions of this work, with respect to the current literature, can be summarized as follows:

- A coordinated distributed secondary control strategy for HMGs is proposed, which treats the HMG as one electrical entity and not as three independent systems (i.e., *ac*, *dc*, and *IC*). The proposed strategy achieve seamless restoration of the variables modified by the primary control at both sides of the HMG, while achieving operation cost minimization.
- The active powers transferred through the *ICs* are considered in the consensus functions and algorithms proposed in this work, which avoids circulating currents and achieves a loss minimization in the *ICs*.
- The viability and effectiveness of the proposed control strategy have been validated through a simulation study using a 33kW HMG.

The rest of the paper is organized as follows. The model of the HMG studied in this work is derived in Section II, and the formulation of the optimization problem is presented in Section III. The distributed secondary control algorithms proposed for HMGs are presented in Section IV. Simulation study and results are extensively discussed in Section V. Finally, Section VI provides some concluding remarks.

II. Hybrid *ac/dc*-Microgrid Modelling

An isolated hybrid *ac/dc*-MG composed of a balanced three-phase *ac*-MG, and a *dc*-MG, interconnected through several *ICs* is considered. A simplified topology for the system under study is presented in Fig. 1, with a set of *ac*-buses $\mathcal{J}_{\rm ac} = \{1, \ldots, J_{\rm ac}\}$, a set of *ac*-DGs $\mathsf{N}_{\rm ac} = \{1, \ldots, N_{\rm ac}\}$, a set of *dc*-buses $\mathcal{J}_{\rm dc} = \{1, \ldots, J_{\rm dc}\}$, a set of *dc*-DGs $\mathsf{N}_{\rm dc} = \{1, \ldots, N_{\rm dc}\}$, and a set of *ICs* $\mathsf{N}_{\rm IC} = \{1, \ldots, N_{\rm IC}\}$. For simplicity, a lumped load is modelled on each side of the HMG (i.e., *ac*-Load $P^{\rm D}_{\rm ac}$ and *dc*-Load $P^{\rm D}_{\rm dc}$), which also includes the line losses. Red arrows show the reference direction of the power flow in the MG: DGs supply power to the system, loads absorb power from the system, and direction of power flow in the *ICs* is taken as positive when power flows from *dc*-side to *ac*-side, and vice versa.

In the *ac*-MG, buses i and j are connected through inductive lines of impedance $Z_{ij} = r_{ij} + jx_{ij}$. On the other hand, in the *dc*-MG, buses j and i are connected through resistive lines of resistance R_{ji}. Generation units (*ac*-DGs and *dc*-DGs) inject real power $P^{\rm G}_{{\rm ac}-i}, P^{\rm G}_{{\rm dc}-j}$ to the MG, which is constrained within minimum and maximum limits. The *ICs* transfer power bidirectionally according to the control set-points, constrained within minimum and maximum limits. The power losses in the k^{th} *IC* $\left(P^{\rm LOSS}_{{\rm IC}-k}\right)$ can be empirically modelled as a fraction of the power through this device [23] $\left(\zeta^{\rm LOSS}_k\,\%\right)$, as follows

$$P^{\rm LOSS}_{{\rm IC}-k} = \zeta^{\rm LOSS}_k P^{\rm ac}_{{\rm IC}-k} \tag{1}$$

Since the modelled *ICs* lack an energy storage unit, the power at both sides of the k^{th} *IC* (and its power losses) are not independent and can be expressed as a function of other variable in the *IC* (e.g., the power $P^{\rm ac}_{{\rm IC}-k}$ or $P^{\rm dc}_{{\rm IC}-k}$). Moreover, only power at one port of the k^{th} *IC* can be controlled. Arbitrarily, in this case, the power in the *ac*-port $P^{\rm ac}_{{\rm IC}-k}$ is the variable to be controlled and it is the variable defined as independent in the *IC*. Then, the variables in the k^{th} *IC* are expressed as shown in (2), where constants $\eta^{\rm IC}_k$ and $\eta^{\rm LOSS}_k$ depend on the direction of power through the *IC*, and are shown in Table I.

TABLE I
Parameters for equation (2).

	Power flow	$\boldsymbol{\eta^{\rm IC}_k}$	$\boldsymbol{\eta^{\rm LOSS}_k}$
$P^{\rm ac}_{{\rm IC}-k} > 0$	from *dc* to *ac*	$\frac{1}{1-\zeta^{\rm LOSS}_k}$	$\frac{\zeta^{\rm LOSS}_k}{1-\zeta^{\rm LOSS}_k}$
$P^{\rm ac}_{{\rm IC}-k} < 0$	from *ac* to *dc*	$1-\zeta^{\rm LOSS}_k$	$-\zeta^{\rm LOSS}_k$

$$P^{\rm dc}_{{\rm IC}-k} = \eta^{\rm IC}_k P^{\rm ac}_{{\rm IC}-k} \tag{2a}$$
$$P^{\rm LOSS}_{{\rm IC}-k} = \eta^{\rm LOSS}_k P^{\rm ac}_{{\rm IC}-k} \tag{2b}$$

Now, from Fig. 1, the following equations can be deduced:

$$P^{\rm ac}_{\rm IC} = P^{\rm D}_{\rm ac} - P^{\rm G}_{\rm ac} \tag{3a}$$
$$P^{\rm dc}_{\rm IC} = P^{\rm G}_{\rm dc} - P^{\rm D}_{\rm dc} \tag{3b}$$

where $P^{\rm G}_{\rm ac} = \sum_{i\in\mathsf{N}_{\rm ac}} P^{\rm G}_{{\rm ac}-i}$ and $P^{\rm G}_{\rm dc} = \sum_{j\in\mathsf{N}_{\rm dc}} P^{\rm G}_{{\rm dc}-j}$ are the total power generated by the *ac*-DGs and *dc*-DGs, respectively, and $P^{\rm ac}_{\rm IC} = \sum_{k\in\mathsf{N}_{\rm IC}} P^{\rm ac}_{{\rm IC}-k}$ and $P^{\rm dc}_{\rm IC} = \sum_{k\in\mathsf{N}_{\rm IC}} P^{\rm dc}_{{\rm IC}-k}$ are the total power at the *ac*-port and *dc*-port, respectively, transferred through the *ICs*.

Now, the total power transferred through multiple *ICs* $(P^{\rm ac}_{\rm IC})$ is defined as a function of the generated powers, as shown in (4). Moreover, the power transferred through each *IC* $\left(P^{\rm ac}_{{\rm IC}-k}\right)$ can be dispatched in order to reduce the losses and, therefore, minimize the operation cost of the HMG.

$$P^{\rm ac}_{\rm IC}(\mathbf{P^G_{ac}}, \mathbf{P^G_{dc}}) = \frac{1}{1+\eta^{\rm IC}}\left(P^{\rm D}_{\rm ac} - P^{\rm G}_{\rm ac} + P^{\rm G}_{\rm dc} - P^{\rm D}_{\rm dc}\right) \tag{4}$$

where $\mathbf{P^G_{ac}} = \{P^{\rm G}_{{\rm ac}-i} : i \in \mathsf{N}_{\rm ac}\}, \mathbf{P^G_{dc}} = \{P^{\rm G}_{{\rm dc}-j} : j \in \mathsf{N}_{\rm dc}\}$ are the set of power generated by the *ac*-DGs and *dc*-DGs, respectively.

III. Optimization Problem Formulation

The optimization problem considered in this work determines the least-cost dispatch of controllable DG and *IC* units in a HMG while maintaining generation and power transfer within limits. Constraints impose the latter condition on DGs power injections and *ICs* power transfer. The formulation is

based on a system representation with constant line losses lumped with the loads as follows:

$$\underset{\mathbf{P^G_{ac}},\mathbf{P^G_{dc}},\mathbf{P^{ac}_{IC}}}{\text{minimize}} \quad \sum_{i\in\mathsf{N}_{\rm ac}} C_i^{\rm ac}\left(P^{\rm G}_{{\rm ac}-i}\right)+\sum_{j\in\mathsf{N}_{\rm dc}} C_j^{\rm dc}\left(P^{\rm G}_{{\rm dc}-j}\right) \tag{5a}$$

$$\text{subject to} \quad P^{\rm D}_{\rm ac}+P^{\rm D}_{\rm dc}+P^{\rm LOSS}_{\rm IC}=P^{\rm G}_{\rm ac}+P^{\rm G}_{\rm dc}, \tag{5b}$$

$$P^{\rm ac}_{\rm IC}=\sum\nolimits_{k\in\mathsf{N}_{\rm IC}} P^{\rm ac}_{{\rm IC}-k}, \tag{5c}$$

$$P^{\rm G-}_{{\rm ac}-i}\le P^{\rm G}_{{\rm ac}-i}\le P^{\rm G+}_{{\rm ac}-i},\quad \forall i\in\mathsf{N}_{\rm ac}, \tag{5d}$$

$$P^{\rm G-}_{{\rm dc}-j}\le P^{\rm G}_{{\rm dc}-j}\le P^{\rm G+}_{{\rm dc}-j},\quad \forall j\in\mathsf{N}_{\rm dc}, \tag{5e}$$

$$P^{\rm ac-}_{{\rm IC}-k}\le P^{\rm ac}_{{\rm IC}-k}\le P^{\rm ac+}_{{\rm IC}-k},\ \forall k\in\mathsf{N}_{\rm IC} \tag{5f}$$

where $C_i^{\rm ac}(P^{\rm G}_{{\rm ac}-i})$ and $C_j^{\rm dc}(P^{\rm G}_{{\rm dc}-j})$ are convex cost functions, $\mathbf{P^{ac}_{IC}}=\{P^{\rm ac}_{{\rm IC}-k}: k\in\mathsf{N}_{\rm IC}\}$ is the set of power transfer through the *ICs*, and $P^{\rm LOSS}_{\rm IC}=\sum_{k\in\mathsf{N}_{\rm IC}} P^{\rm LOSS}_{{\rm IC}-k}$is the total power lost in the *ICs*.

From the optimization problem, (5b) is the power balance constraint, (5c) is the power transfer constraint, and (5d)-(5f) are the power limits constraints. The upper power limits are defined by the superscripts G+ and ac+, while the lower power limits are defined by the superscripts G- and ac-.

The objective function of the optimization problem is strictly convex and the constraints are linear. It is assumed that Slater's constraint qualification condition holds, implying strong duality, and that the problem may be studied through its Lagrange dual. Thus, considering the optimization problem formulated in (5a)-(5f), the Lagrangian function can be written as follows:

$$\begin{aligned}
&\mathsf{L}\big(\mathbf{P^G_{ac}},\mathbf{P^G_{dc}},\mathbf{P^{ac}_{IC}},\lambda^{\rm G},\lambda^{\rm IC},\dots\\
&\quad\dots,\alpha^{+}_{{\rm ac}-i},\alpha^{-}_{{\rm ac}-i},\alpha^{+}_{{\rm dc}-j},\alpha^{-}_{{\rm dc}-j},\alpha^{+}_{{\rm IC}-k},\alpha^{-}_{{\rm IC}-k}\big)\\
&\quad=\sum\nolimits_{i\in\mathsf{N}_{\rm ac}} C_i^{\rm ac}\left(P^{\rm G}_{{\rm ac}-i}\right)+\sum\nolimits_{j\in\mathsf{N}_{\rm dc}} C_j^{\rm dc}\left(P^{\rm G}_{{\rm dc}-j}\right)\\
&\quad+\lambda^{\rm G}\left(P^{\rm D}+P^{\rm LOSS}_{\rm IC}-\sum_{i\in\mathsf{N}_{\rm ac}} P^{\rm G}_{{\rm ac}-i}-\sum_{j\in\mathsf{N}_{\rm dc}} P^{\rm G}_{{\rm dc}-j}\right)\\
&\quad+\lambda^{\rm IC}\left(P^{\rm ac}_{\rm IC}-\sum\nolimits_{k\in\mathsf{N}_{\rm IC}} P^{\rm ac}_{{\rm IC}-k}\right)\\
&\quad+\sum\nolimits_{i\in\mathsf{N}_{\rm ac}} \alpha^{+}_{{\rm ac}-i}\left(P^{\rm G}_{{\rm ac}-i}-P^{\rm G+}_{{\rm ac}-i}\right)\\
&\quad+\sum\nolimits_{i\in\mathsf{N}_{\rm ac}} \alpha^{-}_{{\rm ac}-i}\left(P^{\rm G-}_{{\rm ac}-i}-P^{\rm G}_{{\rm ac}-i}\right)\\
&\quad+\sum\nolimits_{j\in\mathsf{N}_{\rm dc}} \alpha^{+}_{{\rm dc}-j}\left(P^{\rm G}_{{\rm dc}-j}-P^{\rm G+}_{{\rm dc}-j}\right)\\
&\quad+\sum\nolimits_{j\in\mathsf{N}_{\rm dc}} \alpha^{-}_{{\rm dc}-j}\left(P^{\rm G-}_{{\rm dc}-j}-P^{\rm G}_{{\rm dc}-j}\right)\\
&\quad+\sum\nolimits_{k\in\mathsf{N}_{\rm IC}} \alpha^{+}_{{\rm IC}-k}\left(P^{\rm ac}_{{\rm IC}-k}-P^{\rm ac+}_{{\rm IC}-k}\right)\\
&\quad+\sum\nolimits_{k\in\mathsf{N}_{\rm IC}} \alpha^{-}_{{\rm IC}-k}\left(P^{\rm ac-}_{{\rm IC}-k}-P^{\rm ac}_{{\rm IC}-k}\right)
\end{aligned} \tag{6}$$

where the Lagrange multiplier $\lambda^{\rm G}$ is associated with the power balance constraint (5b), $\lambda^{\rm IC}$ with the power transfer constraint (5c), $\{\alpha^{+}_{{\rm ac}-i},\alpha^{-}_{{\rm ac}-i},\alpha^{+}_{{\rm dc}-j},\alpha^{-}_{{\rm dc}-j}\}$ with the maximum and minimum power outputs of DGs in equations (5d)-(5e), and $\{\alpha^{+}_{{\rm IC}-k},\alpha^{-}_{{\rm IC}-k}\}$ with the power limits of the *ICs* in equation (5f). Now, using (2) and (4), the KKT optimality conditions of the optimization problem are as follows:

Stationary condition :

$$\begin{aligned}
\frac{\partial\mathsf{L}}{\partial P^{\rm G}_{{\rm ac}-i}}&=0=\nabla C_i^{\rm ac}\left(P^{\rm G}_{{\rm ac}-i}\right)-\lambda^{\rm G}\left(\frac{2\eta^{\rm IC}}{\eta^{\rm IC}+1}\right)\\
&\quad-\lambda^{\rm IC}\left(\frac{1}{\eta^{\rm IC}+1}\right)+\alpha^{+}_{{\rm ac}-i}-\alpha^{-}_{{\rm ac}-i},\ i\in\mathsf{N}_{\rm ac}
\end{aligned} \tag{7a}$$

$$\begin{aligned}
\frac{\partial\mathsf{L}}{\partial P^{\rm G}_{{\rm dc}-j}}&=0=\nabla C_j^{\rm dc}\left(P^{\rm G}_{{\rm dc}-j}\right)-\lambda^{\rm G}\left(\frac{2}{\eta^{\rm IC}+1}\right)\\
&\quad+\lambda^{\rm IC}\left(\frac{1}{\eta^{\rm IC}+1}\right)+\alpha^{+}_{{\rm dc}-j}-\alpha^{-}_{{\rm dc}-j},\ j\in\mathsf{N}_{\rm dc}
\end{aligned} \tag{7b}$$

$$\begin{aligned}
\frac{\partial\mathsf{L}}{\partial P^{\rm ac}_{{\rm IC}-k}}&=0=\lambda^{\rm G}\eta^{\rm LOSS}_k-\lambda^{\rm IC}\left(\frac{P^{\rm ac}_{{\rm IC}-k}-P^{\rm ac}_{\rm IC}}{P^{\rm ac}_{{\rm IC}-k}}\right)\\
&\quad+\alpha^{+}_{{\rm IC}-k}-\alpha^{-}_{{\rm IC}-k},\qquad k\in\mathsf{N}_{\rm IC}
\end{aligned} \tag{7c}$$

Complementary slackness

$$\alpha^{+}_{{\rm ac}-i}\left(P^{\rm G}_{{\rm ac}-i}-P^{\rm G+}_{{\rm ac}-i}\right)=0,\quad i\in\mathsf{N}_{\rm ac} \tag{7d}$$

$$\alpha^{-}_{{\rm ac}-i}\left(P^{\rm G-}_{{\rm ac}-i}-P^{\rm G}_{{\rm ac}-i}\right)=0,\quad i\in\mathsf{N}_{\rm ac} \tag{7e}$$

$$\alpha^{+}_{{\rm dc}-j}\left(P^{\rm G}_{{\rm dc}-j}-P^{\rm G+}_{{\rm dc}-j}\right)=0,\quad j\in\mathsf{N}_{\rm dc} \tag{7f}$$

$$\alpha^{-}_{{\rm dc}-j}\left(P^{\rm G-}_{{\rm dc}-j}-P^{\rm G}_{{\rm dc}-j}\right)=0,\quad j\in\mathsf{N}_{\rm dc} \tag{7g}$$

$$\alpha^{+}_{{\rm IC}-k}\left(P^{\rm ac}_{{\rm IC}-k}-P^{\rm ac+}_{{\rm IC}-k}\right)=0,\quad k\in\mathsf{N}_{\rm IC} \tag{7h}$$

$$\alpha^{-}_{{\rm IC}-k}\left(P^{\rm ac-}_{{\rm IC}-k}-P^{\rm ac}_{{\rm IC}-k}\right)=0,\quad k\in\mathsf{N}_{\rm IC} \tag{7i}$$

Primal feasibility :

(5b), (5c), (5d), (5e) and (5f)

Dual feasibility :

$$\alpha^{+}_{{\rm ac}-i},\alpha^{-}_{{\rm ac}-i},\alpha^{+}_{{\rm dc}-j},\alpha^{-}_{{\rm dc}-j},\alpha^{+}_{{\rm IC}-k},\alpha^{-}_{{\rm IC}-k}\ge 0 \tag{7j}$$

Note that for each $i\in\mathsf{N}_{\rm ac}$ and $j\in\mathsf{N}_{\rm dc}$, (7a) and (7b) can each be solved respectively to obtain the Lagrange multiplier $\lambda^{\rm G}$, while for each $k\in\mathsf{N}_{\rm IC}$, (7c) can be solved to obtain the Lagrange multiplier $\lambda^{\rm IC}$; as useful notation, the corresponding solutions are denoted as

$$\lambda^{\rm G}_{{\rm ac}-i}\coloneqq\frac{\eta^{\rm IC}+1}{2\eta^{\rm IC}}\left(\nabla C_i^{\rm ac}\left(P^{\rm G}_{{\rm ac}-i}\right)+\alpha^{+}_{{\rm ac}-i}-\alpha^{-}_{{\rm ac}-i}\right)-\frac{\lambda^{\rm IC}}{2\eta^{\rm IC}} \tag{8a}$$

$$\lambda^{\rm G}_{{\rm dc}-j}\coloneqq\frac{\eta^{\rm IC}+1}{2}\left(\nabla C_j^{\rm dc}\left(P^{\rm G}_{{\rm dc}-j}\right)+\alpha^{+}_{{\rm dc}-j}-\alpha^{-}_{{\rm dc}-j}\right)+\frac{\lambda^{\rm IC}}{2} \tag{8b}$$

$$\lambda^{\rm IC}_k\coloneqq\frac{P^{\rm ac}_{{\rm IC}-k}\left[\left(\eta^{\rm IC}_k-1\right)\lambda^{\rm G}+\alpha^{+}_{{\rm IC}-k}-\alpha^{-}_{{\rm IC}-k}\right]}{P^{\rm ac}_{{\rm IC}-k}-P^{\rm ac}_{\rm IC}} \tag{8c}$$

where, by optimality, (9a) and (9b) must hold.

$$\lambda^{\rm G}=\lambda^{\rm G}_{{\rm ac}-i}=\lambda^{\rm G}_{{\rm dc}-j},\quad \forall i\in\mathsf{N}_{\rm ac},\ \forall j\in\mathsf{N}_{\rm dc} \tag{9a}$$

$$\lambda^{\rm IC}=\lambda^{\rm IC}_k,\qquad \forall k\in\mathsf{N}_{\rm IC} \tag{9b}$$

We can interpret $\lambda^{\rm G}_{{\rm ac}-i}$ as a Lagrange multiplier for the i^{th} DG on the *ac*-side, $\lambda^{\rm G}_{{\rm dc}-j}$ as a Lagrange multiplier for the j^{th} DG on the *dc*-side, and $\lambda^{\rm IC}_k$ as a Lagrange multiplier of the k^{th} *IC*. Based on the optimality conditions of the OD problem, a distributed control strategy is designed with the objective of providing secondary variables regulation (i.e., frequency and voltage regulation in the *ac*-MG, and voltage regulation in the *dc*-MG), while driving the HMG with multiple *ICs* to an OD that complies with the KKT conditions (7).

IV. Proposed Distributed Secondary Control

The distributed control scheme proposed in this section aims to regulate the secondary variables in a HMG, while maintaining optimality of dispatch. The control scheme is designed for the three components of the HMG. On the other hand, the design of the control scheme is based on the convex optimization problem (5a)-(5f) presented in Section III. The required communication network and the control strategies proposed for DGs and *ICs* are explained in the following.

A. Communication Structure Requirements

A communication network is required for the implementation of the proposed distributed controller. The distributed bidirectional communication network is modelled by an undirected graph $G(\mathcal{V}, \mathcal{E}, A)$ where $\mathcal{V} = \{1, \ldots, n\}$ is a labeling of the DGs, $\mathcal{E} \subseteq \mathcal{V} \times \mathcal{V}$ is the set of communication links, and $\mathbf{A}$ is the $n \times n$ *weighted adjacency matrix* of the graph, with elements $a_{ij} = a_{ji} \geq 0$. Particularly, it is considered that $(i, j) \in \mathcal{E}$ if node *i* sends information directly to node *j*, and in this case, $a_{ij} > 0$ [24]. Thus, the sparsity pattern of the adjacency matrix $\mathbf{A}$ encodes the topology of the communication layer.

Let $x_i \in \mathsf{R}$ denote the value of some quantity of interest at bus i; in our specific context, x_i will be an internal controller variable. It is said the variables x_i achieve consensus if $x_i(t) - x_j(t) \to 0$ as $t \to \infty$. If the $\mathbf{A}$ matrix have a spanning tree, i.e., there is a path from any single node to any other one in the communication graph, consensus can be achieved via the following algorithm [26]:

$$\dot{x}_i = -\sum\nolimits_{j \in \mathsf{N}(i)} a_{ij} \left(x_i - x_j\right) \tag{10}$$

B. Control scheme proposed for the ac-DGs

The control scheme proposed for the *ac*-DGs is responsible for regulating the frequency on the *ac*-side, while minimizing the operation cost of all the DGs in the HMG. It is given by

$$\omega_i = \omega^* + M_{\mathrm{ac}-i} P^{\mathrm{G}}_{\mathrm{ac}-i} + \Omega^{\mathrm{G}}_{\mathrm{ac}-i} \tag{11a}$$

$$\dot{\Omega}^{\mathrm{G}}_{\mathrm{ac}-i} = -k^a_{\mathrm{ac}-i} \left(\omega_i - \omega^*\right) + \Lambda^{\mathrm{ac}}_{\mathrm{ac}-i} + \Lambda^{\mathrm{dc}}_{\mathrm{ac}-i} \tag{11b}$$

$$\Lambda^{\mathrm{ac}}_{\mathrm{ac}-i} = -k^b_{\mathrm{ac}-i} \sum\nolimits_{j \in \mathsf{N}_{\mathrm{ac}}} a_{ij} \left(\lambda^{\mathrm{G}}_{\mathrm{ac}-i} - \lambda^{\mathrm{G}}_{\mathrm{ac}-j}\right) \tag{11c}$$

$$\Lambda^{\mathrm{dc}}_{\mathrm{ac}-i} = -k^c_{\mathrm{ac}-i} \sum\nolimits_{j \in \mathsf{N}_{\mathrm{dc}}} a_{ij} \left(\lambda^{\mathrm{G}}_{\mathrm{ac}-i} - \lambda^{\mathrm{G}}_{\mathrm{dc}-j}\right) \tag{11d}$$

$$\dot{\alpha}^{+}_{\mathrm{ac}-i} = \mu^a_{\mathrm{ac}-i} \max\left\{ P^{\mathrm{G}}_{\mathrm{ac}-i} - P^{\mathrm{G}+}_{\mathrm{ac}-i} + \frac{k^d_{\mathrm{ac}-i}}{\mu^a_{\mathrm{ac}-i}} \alpha^{+}_{\mathrm{ac}-i}, 0 \right\} - k^d_{\mathrm{ac}-i} \alpha^{+}_{\mathrm{ac}-i} \tag{11e}$$

$$\dot{\alpha}^{-}_{\mathrm{ac}-i} = \mu^b_{\mathrm{ac}-i} \max\left\{ P^{\mathrm{G}-}_{\mathrm{ac}-i} - P^{\mathrm{G}}_{\mathrm{ac}-i} + \frac{k^e_{\mathrm{ac}-i}}{\mu^b_{\mathrm{ac}-i}} \alpha^{-}_{\mathrm{ac}-i}, 0 \right\} - k^e_{\mathrm{ac}-i} \alpha^{-}_{\mathrm{ac}-i} \tag{11f}$$

$$\lambda^{\mathrm{G}}_{\mathrm{ac}-i} = \frac{\hat{\eta}^{\mathrm{IC}}_i + 1}{2\hat{\eta}^{\mathrm{IC}}_i} \left(\nabla C^{\mathrm{ac}}_i \left(P^{\mathrm{G}}_{\mathrm{ac}-i}\right) + \alpha^{+}_{\mathrm{ac}-i} - \alpha^{-}_{\mathrm{ac}-i}\right) - \frac{1}{2\hat{\eta}^{\mathrm{IC}}_i} \hat{\lambda}^{\mathrm{IC}}_i \tag{11g}$$

A block diagram of the proposed controller is presented in Fig. 2a. The reactive power injections are not considered in the formulation of the optimization problem since it is assumed that the *ac*-DSC described in [25] controls reactive power injections to regulate voltages in the *ac*-MG. Thus, the proposed scheme focuses on frequency and *dc*-voltage control by means of optimally dispatching of real power of DG units.

The term $\Omega^{\mathrm{G}}_{\mathrm{ac}-i}$ in (11a) is a secondary control action to drive the units to their OD level. Specifically, the frequency droop controller in (11a) is perturbed by the control action $\Omega^{\mathrm{G}}_{\mathrm{ac}-i}$, in order to change the dispatch of the *ac*-DGs until all DGs satisfy the consensus condition (9a), which corresponds to the (unique) dual variable associated with the demand-supply balance equation of the HMG's OD problem, (5b).

The $\lambda^{\mathrm{G}}_{\mathrm{ac}-i}$ of each *ac*-DG that complies with the stationarity condition is calculated from (11g). Variables $\alpha^{+}_{\mathrm{ac}-i}$ and $\alpha^{-}_{\mathrm{ac}-i}$ are local control actions to keep the active power dispatch of *ac*-DGs within limits, which in equilibrium correspond to the dual variables associated with maximum and minimum power limits, respectively. The control actions $\alpha^{+}_{\mathrm{ac}-i}$ and $\alpha^{-}_{\mathrm{ac}-i}$ are obtained from (11e) and (11f), respectively. In these equations, an increase in the values of the control actions is induced whenever *ac*-DG$_i$ goes beyond its maximum or minimum active power dispatch levels. Also, control actions $\alpha^{+}_{\mathrm{ac}-i}$ and $\alpha^{-}_{\mathrm{ac}-i}$ are driven down to zero by the controller if the active power dispatch of *ac*-DG$_i$ is strictly within limits. In (11b)-(11f), $k^{\{a,b,c,d,e\}}_{\mathrm{ac}-i}$, $\mu^{\{a,b\}}_{\mathrm{ac}-i}$ are positive gains which can be used to adjust the dynamic response of the proposed algorithm.

The calculation of $\lambda^{\mathrm{G}}_{\mathrm{ac}-i}$ in (11g) requires information from the *ICs* (variables $\hat{\eta}^{\mathrm{IC}}_j$ and $\hat{\lambda}^{\mathrm{IC}}_j$). However, it is not mandatory for all the *ac*-DGs to be communicated with (at least) one *IC*. Therefore, a distributed estimator is proposed. The estimate of the variables from the *ICs* (i.e., $\hat{\eta}^{\mathrm{IC}}_j$ and $\hat{\lambda}^{\mathrm{IC}}_j$) are calculated with the distributed observers shown in (12), where variables $\hat{\eta}^{\mathrm{IC}}_k$ and λ^{IC}_k are received from the *ICs* communicating with *ac*-DG$_i$. The term λ^{IC} corresponds to the (unique) dual variable associated with the power transfer through the *ICs* (5c).

$$\dot{\hat{\eta}}^{\mathrm{IC}}_i = -\sum_{j \in \mathsf{N}} a_{ij} \left(\hat{\eta}^{\mathrm{IC}}_i - \hat{\eta}^{\mathrm{IC}}_j\right) - \sum_{k \in \mathsf{N}_{\mathrm{IC}}} a_{ik} \left(\hat{\eta}^{\mathrm{IC}}_i - \hat{\eta}^{\mathrm{IC}}_k\right) \tag{12a}$$

$$\dot{\hat{\lambda}}^{\mathrm{IC}}_i = -\sum_{j \in \mathsf{N}} a_{ij} \left(\hat{\lambda}^{\mathrm{IC}}_i - \hat{\lambda}^{\mathrm{IC}}_j\right) - \sum_{k \in \mathsf{N}_{\mathrm{IC}}} a_{ik} \left(\hat{\lambda}^{\mathrm{IC}}_i - \lambda^{\mathrm{IC}}_k\right) \tag{12b}$$

In (12), $\mathsf{N} = \{\mathsf{N}_{\mathrm{ac}}, \mathsf{N}_{\mathrm{dc}}\}$. The variables sent/received by the *ac*-DGs are summarized in Table II.

TABLE II
Data transferred between agents.

	To *ac*-DGs	To *dc*-DGs	To *ICs*
From *ac*-DG$_i$	$\lambda^{\mathrm{G}}_{\mathrm{ac}-i}$	$\lambda^{\mathrm{G}}_{\mathrm{ac}-i}$	$\lambda^{\mathrm{G}}_{\mathrm{ac}-i}$
From *dc*-DG$_j$	$\lambda^{\mathrm{G}}_{\mathrm{dc}-j}$	$\lambda^{\mathrm{G}}_{\mathrm{dc}-j}$	$\lambda^{\mathrm{G}}_{\mathrm{dc}-j}$
From IC_k	$\lambda^{\mathrm{IC}}_k, \eta^{\mathrm{IC}}$	$\lambda^{\mathrm{IC}}_k, \eta^{\mathrm{IC}}$	$\lambda^{\mathrm{IC}}_k, \hat{P}^{\mathrm{ac}}_{\mathrm{IC}-k}, \hat{P}^{\mathrm{dc}}_{\mathrm{IC}-k}$

C. Control scheme proposed for the dc-DGs

The control scheme proposed for the *dc*-DGs is responsible for regulating the voltage of the *dc*-side of the MG, while

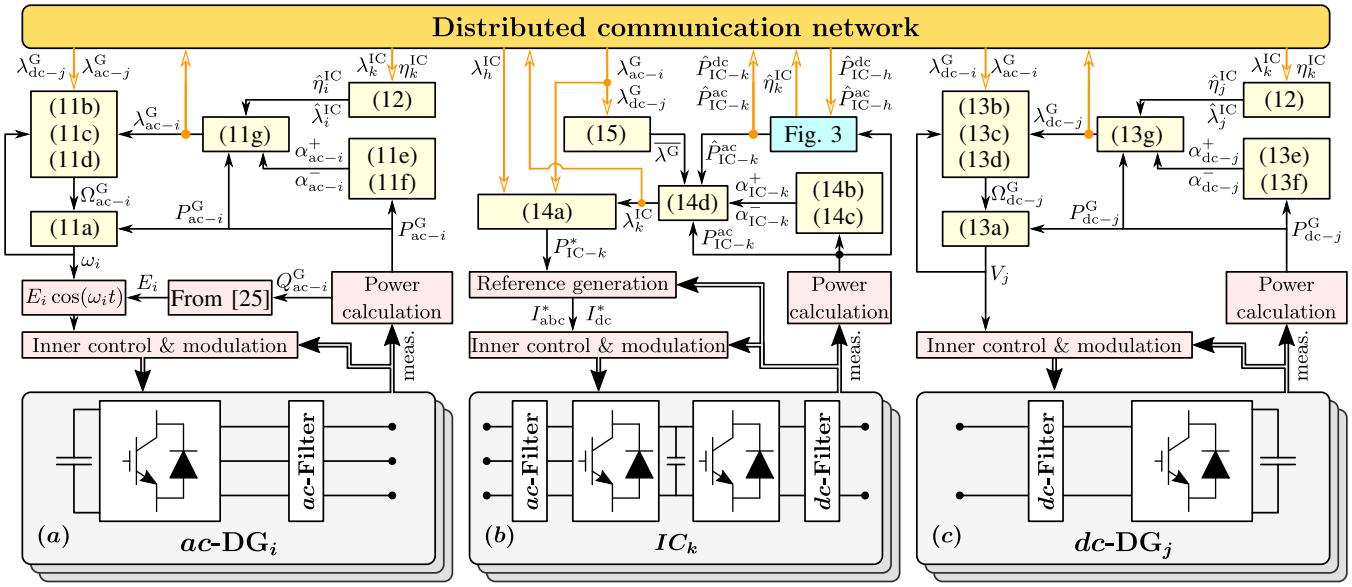

Fig. 2. Proposed distributed secondary control for: (a) *ac*-MG (*ac*-DSC), (b) *IC* (*IC* DSC), (c) *dc*-MG (*dc*-DSC).

minimizing the operation cost of all the DGs in the HMG (13). It is given by

$$V_j = V^* + M_{\mathrm{dc}-j} P^{\mathrm{G}}_{\mathrm{dc}-j} + \Omega^{\mathrm{G}}_{\mathrm{dc}-j} \tag{13a}$$

$$\dot{\Omega}^{\mathrm{G}}_{\mathrm{dc}-j} = -k^a_{\mathrm{dc}-j}\left(V_j - V^*\right) + \Lambda^{\mathrm{dc}}_{\mathrm{dc}-i} + \Lambda^{\mathrm{ac}}_{\mathrm{dc}-i} \tag{13b}$$

$$\Lambda^{\mathrm{dc}}_{\mathrm{dc}-i} = -k^b_{\mathrm{dc}-j} \sum\nolimits_{i\in \mathtt{N}_{\mathrm{dc}}} a_{ji}\left(\lambda^{\mathrm{G}}_{\mathrm{dc}-j} - \lambda^{\mathrm{G}}_{\mathrm{dc}-i}\right) \tag{13c}$$

$$\Lambda^{\mathrm{ac}}_{\mathrm{dc}-i} = -k^c_{\mathrm{dc}-j} \sum\nolimits_{i\in \mathtt{N}_{\mathrm{ac}}} a_{ji}\left(\lambda^{\mathrm{G}}_{\mathrm{dc}-j} - \lambda^{\mathrm{G}}_{\mathrm{ac}-i}\right) \tag{13d}$$

$$\dot{\alpha}^+_{\mathrm{dc}-j} = \mu^a_{\mathrm{dc}-j} \max\left\{P^{\mathrm{G}}_{\mathrm{dc}-j} - P^{\mathrm{G}+}_{\mathrm{dc}-j} + \frac{k^d_{\mathrm{dc}-j}}{\mu^a_{\mathrm{dc}-j}}\alpha^+_{\mathrm{dc}-j}, 0\right\} - k^d_{\mathrm{dc}-j}\alpha^+_{\mathrm{dc}-j} \tag{13e}$$

$$\dot{\alpha}^-_{\mathrm{dc}-j} = \mu^b_{\mathrm{dc}-j} \max\left\{P^{\mathrm{G}-}_{\mathrm{dc}-j} - P^{\mathrm{G}}_{\mathrm{dc}-j} + \frac{k^e_{\mathrm{dc}-j}}{\mu^b_{\mathrm{dc}-j}}\alpha^-_{\mathrm{dc}-j}, 0\right\} - k^e_{\mathrm{dc}-j}\alpha^-_{\mathrm{dc}-j} \tag{13f}$$

$$\lambda^{\mathrm{G}}_{\mathrm{dc}-j} = \frac{\hat{\eta}^{\mathrm{IC}}_j + 1}{2}\left(\nabla C^{\mathrm{dc}}_j\left(P^{\mathrm{G}}_{\mathrm{dc}-j}\right) + \alpha^+_{\mathrm{dc}-j} - \alpha^-_{\mathrm{dc}-j}\right) + \frac{1}{2}\hat{\lambda}^{\mathrm{IC}}_j \tag{13g}$$

A block diagram of the controller is shown in Fig. 2c. The term $\Omega^{\mathrm{G}}_{\mathrm{dc}-j}$ in (13a) is a secondary control action to drive the units to their OD level. Precisely, the voltage droop controller in (13a) is perturbed by the control action $\Omega^{\mathrm{G}}_{\mathrm{dc}-j}$, to change the dispatch of the *dc*-DGs until all DGs satisfy the consensus condition (9a), which corresponds to the (unique) dual variable associated with the demand-supply balance equation of the HMG's OD problem, (5b).

The $\lambda^{\mathrm{G}}_{\mathrm{dc}-j}$ of each *dc*-DG that complies with the stationarity condition can be calculated from (13g). Variables $\alpha^+_{\mathrm{dc}-j}$ and $\alpha^-_{\mathrm{dc}-j}$ are local control actions to keep the active power dispatch of *dc*-DGs within limits, which in equilibrium correspond to the dual variables associated with maximum and minimum active power limits, respectively. The control actions $\alpha^+_{\mathrm{dc}-j}$ and $\alpha^-_{\mathrm{dc}-j}$ are obtained from equations (13e) and (13f), respectively. In these equations, an increase in the values of the control actions is induced whenever *dc*-DG$_i$ goes beyond its maximum or minimum active power dispatch levels. Also, control actions $\alpha^+_{\mathrm{dc}-j}$ and $\alpha^-_{\mathrm{dc}-j}$ are driven down to zero by the controller if the active power dispatch of *dc*-DG$_j$ is strictly within limits. In (13b)-(13f), $k^{\{a,b,c,d,e\}}_{\mathrm{dc}-j}$ and $\mu^{\{a,b\}}_{\mathrm{dc}-i}$ are positive gains of the controllers. The variables sent/received by the *dc*-DGs are summarized in Table II.

D. Control scheme proposed for the ICs

In addition to contributing to the minimization of the operation cost by transferring power between the two sides of the HMG, the *ICs* must dispatch the power transferred through them in order to reduce the losses in the *ac*-to-*dc* (and vice-versa) conversion and, therefore, help reaching the OD point. The controller shown in Fig. 2b is proposed for achieving the aforementioned control tasks based on (14).

$$\dot{P}^*_{\mathrm{IC}-k} = -\tau^a_{\mathrm{IC}-k} \sum\nolimits_{i\in \mathtt{N}_{\mathrm{ac}}} \sum\nolimits_{j\in \mathtt{N}_{\mathrm{dc}}} a_{ik}a_{jk}\left(\lambda^{\mathrm{G}}_{\mathrm{ac}-i} - \lambda^{\mathrm{G}}_{\mathrm{dc}-j}\right) - \tau^b_{\mathrm{IC}-k} \sum\nolimits_{h\in \mathtt{N}_{\mathrm{IC}}} a_{kh}\left(\lambda^{\mathrm{IC}}_k - \lambda^{\mathrm{IC}}_h\right) \tag{14a}$$

$$\dot{\alpha}^+_{\mathrm{IC}-k} = \mu^a_{\mathrm{IC}-k} \max\left\{P^{\mathrm{ac}}_{\mathrm{IC}-k} - P^{\mathrm{ac}+}_{\mathrm{IC}-k} + \frac{\tau^a_{\mathrm{IC}-k}}{\mu^a_{\mathrm{IC}-k}}\alpha^+_{\mathrm{IC}-k},\ 0\right\} - \tau^a_{\mathrm{IC}-k}\alpha^+_{\mathrm{IC}-k} \tag{14b}$$

$$\dot{\alpha}^-_{\mathrm{IC}-k} = \mu^b_{\mathrm{IC}-k} \max\left\{P^{\mathrm{ac}-}_{\mathrm{IC}-k} - P^{\mathrm{ac}}_{\mathrm{IC}-k} + \frac{\tau^b_{\mathrm{IC}-k}}{\mu^b_{\mathrm{IC}-k}}\alpha^-_{\mathrm{IC}-k},\ 0\right\} - \tau^b_{\mathrm{IC}-k}\alpha^-_{\mathrm{IC}-k} \tag{14c}$$

$$\lambda^{\mathrm{IC}}_k = \frac{P^{\mathrm{ac}}_{\mathrm{IC}-k}}{P^{\mathrm{ac}}_{\mathrm{IC}-k} - P^{\mathrm{ac}}_{\mathrm{IC}}}\left[\left(\eta^{\mathrm{IC}}_k - 1\right)\overline{\lambda^{\mathrm{G}}} + \alpha^+_{\mathrm{IC}-k} - \alpha^-_{\mathrm{IC}-k}\right] \tag{14d}$$

In (14a)-(14d), $P^*_{\mathrm{IC}-k}$ is the power through the k^{th} *IC*, which is positive when transferred from the *dc*-side to the

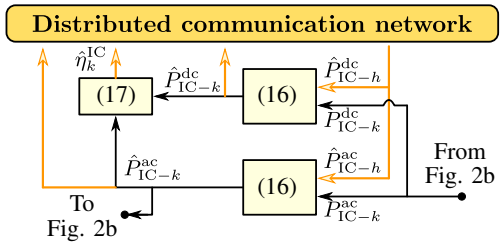

Fig. 3. Block diagram for the estimator implemented in the *ICs*.

ac-side, and negative in the opposite direction, and $\overline{\lambda^{\mathrm{G}}}$ is the average value of the variables $\lambda^{\mathrm{G}}_{\mathrm{ac}-i}$ and $\lambda^{\mathrm{G}}_{\mathrm{dc}-j}$ received from the DGs communicating with IC_k, as follows

$$\overline{\lambda^{\mathrm{G}}} = \frac{\sum_{i\in \mathsf{N}_{\mathrm{ac}}} a_{ik}\lambda^{\mathrm{G}}_{\mathrm{ac}-i} + \sum_{j\in \mathsf{N}_{\mathrm{dc}}} a_{jk}\lambda^{\mathrm{G}}_{\mathrm{dc}-j}}{\sum_{i\in \mathsf{N}_{\mathrm{ac}}} a_{ik} + \sum_{j\in \mathsf{N}_{\mathrm{dc}}} a_{jk}} \tag{15}$$

The control actions $\alpha^{+}_{\mathrm{IC}-k}$ and $\alpha^{-}_{\mathrm{IC}-k}$ are local control actions to keep the active power transferred through IC_k within limits, which in equilibrium correspond to the dual variables associated with maximum and minimum active power limits, respectively. The first term at the right-hand side in (14a) produces a power transfer from the cheaper side to the more expensive side by comparing the values of $\lambda^{\mathrm{G}}_{\mathrm{ac}-i}$ and $\lambda^{\mathrm{G}}_{\mathrm{dc}-j}$. The second term at the right-hand side in (14a) changes the dispatch of the *ICs* until they satisfy the consensus condition (9b), which corresponds to the (unique) dual variable associated with the power transfer equation of the HMG's OD problem, (5c).

The constant η^{IC} that relates the total power at the *ac*-side of the *ICs* to that at the *dc*-side of the *ICs* must be known by the *ac*-DGs (11g) and *dc*-DGs (13g). This constant can be easily calculated in a HMG with a single *IC* using (2a). However, this calculation is more complicated when multiple *ICs* and a distributed communication network are considered since each *IC* does not know the amount of power being transferred through all the others.

In this case, the total power transferred through the *ICs* in a HMG can be estimated with local information from IC_k ($k \in \mathsf{N}_{\mathrm{IC}}$) and its neighbouring *ICs* [26]–[28], as shown in Fig. 3. Let $\hat{\Gamma}_k$ be the estimate of the variable Γ (e.g., the total power transferred through the *ICs* at the *ac*-side $P^{\mathrm{ac}}_{\mathrm{IC}}$ or the *dc*-side $P^{\mathrm{dc}}_{\mathrm{IC}}$), γ_k be the local variable ($P^{\mathrm{ac}}_{\mathrm{IC}-k}$ or $P^{\mathrm{dc}}_{\mathrm{IC}-k}$), a_{kh} be the element of the adjacency matrix which represent the communication channel between IC_k and IC_h ($k, h \in \mathsf{N}_{\mathrm{IC}}$), and g be the total number of *ICs* in the HMG. Then, the total power transferred through the *ICs* can be estimated with a distributed observer [27], as follows:

$$\hat{\Gamma}_k = g\cdot\gamma_k - \int \sum\nolimits_{h\in \mathsf{N}_{\mathrm{IC}}} a_{kh}\left(\hat{\Gamma}_k(\tau) - \hat{\Gamma}_h(\tau)\right) d\tau \tag{16}$$

Therefore, the constant $\hat{\eta}^{\mathrm{IC}}_k$ for implementing the controllers proposed in (11g) and (13g) is calculated as shown in (17). Moreover, the total power transferred at the *ac*-side of the *ICs* needed in (14d) is estimated using (16).

$$\hat{\eta}^{\mathrm{IC}}_k = \hat{P}^{\mathrm{dc}}_{\mathrm{IC}-k}/\hat{P}^{\mathrm{ac}}_{\mathrm{IC}-k}, \qquad \forall k \in \mathsf{N}_{\mathrm{IC}} \tag{17}$$

The variables exchanged by the *ICs* are shown in Table II.

In this way, the controller proposed in sections IV-B, IV-C and IV-D, drives the system to an OD point, i.e., it complies with the KKT conditions of the optimization problem. In steady-state, the optimality condition (9a) is enforced by (11b), (13b) and (14a).

V. Simulation Results

In order to validate the proposed control strategy, its performance is assessed in a case study using the HMG configuration presented in the online Appendix A [29]. The simulated system is composed of fifteen units: six *ac*-DGs composing the *ac*-MG, six *dc*-DGs composing the *dc*-MG, and three *ICs* for interconnecting the *ac*-MG and the *dc*-MG. The nominal voltage in the *ac*-MG is 415V@50Hz (phase-to-phase RMS voltage), while in the *dc*-MG the nominal voltage is 400V.

A. Test #1: Operation Test

In this test, different parts of the controller are sequentially enabled in order to highlight the effect of different terms within the control scheme. The local-load of the 12 DGs remains constant, as summarized in Table III. The total load of the HMG is 24.6kW (9.9kW on *dc*-side and 14.7kW on *ac*-side), i.e., 74.5% of the nominal active power (33.0kW). The load power on the *dc*-side ($R_1, \ldots, R_6$) is 66.0% of the nominal power of this side (15.0kW); meanwhile, the active load power on the *ac*-side ($Z_1, \ldots, Z_6$) corresponds to 81.7% of 18.0kW. The reactive power loads are not considered since the proposed control strategy is not affecting the reactive power on the *ac*-MG. The results for this test are shown in Fig. 4 and Fig. 5.

TABLE III
HYBRID *ac/dc*-MG, BASE LOAD CONDITIONS.

Load	***kW***	**Load**	***kW***	**Load**	***kW***	**Load**	***kW***
R_1	0.9	R_4	2.4	Z_1	2.5	Z_4	2.4
R_2	1.3	R_5	1.5	Z_2	1.7	Z_5	2.1
R_3	2.1	R_6	1.7	Z_3	2.3	Z_6	3.7

The simulation starts with the inner, primary and secondary controllers enabled. Regarding the distributed secondary control loop, only the optimization within each MG considering the operation limits constraints and the restoring terms are enabled (independently).

For $0s < t < 50s$, the DGs are operating within limits (see Fig. 4a for $P^{\mathrm{G}}_{\mathrm{ac}-i}$ and Fig. 4d for $P^{\mathrm{G}}_{\mathrm{dc}-j}$), and the Lagrange multipliers associated with the power limits constraint are zero (see Fig. 4b for $\alpha^{+}_{\mathrm{ac}-i}$ and Fig. 4e for $\alpha^{+}_{\mathrm{dc}-j}$). The secondary variables are properly regulated (see Fig. 4c for frequency and Fig. 4f for *dc*-voltage). On the other hand, the power through the *ICs* is zero (see Fig. 5a) and, therefore, the losses in the *ICs* are also zero (see Fig. 5c). The λ^{G} consensus is achieved within each MG (see Fig. 5e) and the total operating cost is shown in Fig. 5d [$C_T = 820.55$ ($/h$)].

At $t = 50s$, optimization among all the DGs is enabled. On the other hand, the λ^{IC} consensus and the *ICs* limits constraints are maintained deactivated.

Enabling the λ^{G} consensus produces an increase in the power generated in the cheaper MG (*dc*-MG, see Fig. 4d)

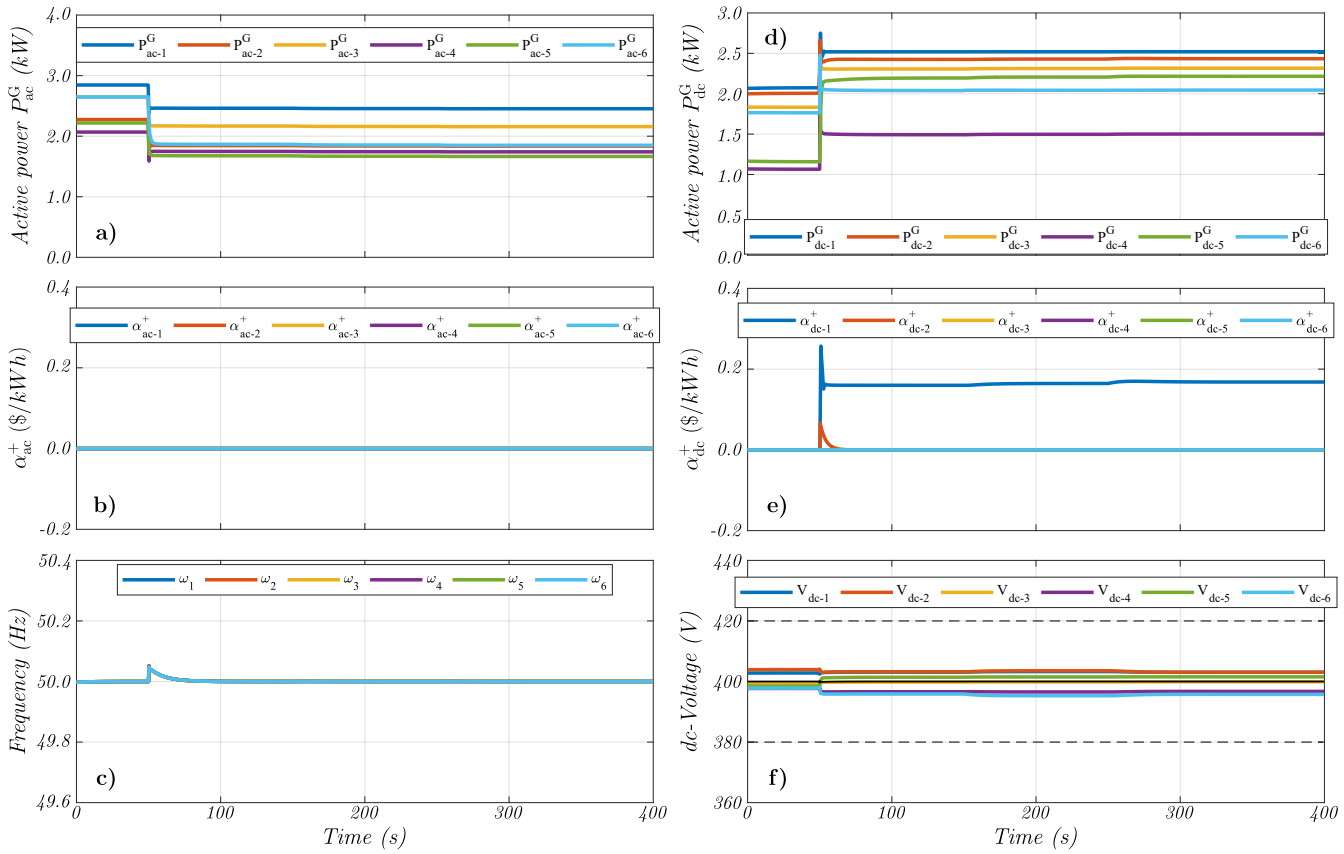

Fig. 4. Simulation Test #1: (a)&(d) Active power generated by *ac*-DGs ($P^{\mathrm{G}}_{\mathrm{ac}-i}$) and *dc*-DGs ($P^{\mathrm{G}}_{\mathrm{dc}-j}$), respectively. (b)&(e) Lagrange multiplier for generated power constraints ($\alpha^{+}_{\mathrm{ac}-i}$ and $\alpha^{+}_{\mathrm{dc}-j}$). (c)&(f) Secondary variables (frequency and *dc*-voltage).

and a decrease in that of the more expensive one (*ac*-MG, see Fig. 4a). Furthermore, *dc*-DG$_1$ and *dc*-DG$_2$ touch the upper power limit but, in steady-state, only the former one is fixed at the maximum value ($P^{\mathrm{G}}_{\mathrm{dc}-1} = P^{\mathrm{G}+}_{\mathrm{dc}-1} = 2.5kW$), as explained by the Lagrange multiplier associated with the limits constraint (see Fig. 4e). The secondary variables are maintained within limits after the transient (see Fig. 4c for frequency and Fig. 4f for *dc*-voltage).

Since the power through the *ICs* flows from the *dc*-MG to the *ac*-MG, the power transfer is positive, as depicted in Fig. 5a. On the other hand, since the λ^{IC} consensus is not active (see Fig. 5f), the *ICs* only share the power for achieving λ^{G} consensus. In this scenario, all the *ICs* are operating within limits and the Lagrange multiplier associated with this constraint is zero (see Fig. 5b). The total operating cost of the MG is reduced when activating the optimization among DGs [$C_T = 819.55$ ($/h$), see Fig. 5d].

The λ^{IC} consensus is activated at $t = 150s$. The *ICs* begin to work collaboratively and they reach the same value of λ^{IC}, as depicted in Fig. 5f. Moreover, a re-dispatch of the power through the *ICs* is produced (see Fig. 5a) and, therefore, the losses in the *ICs* change as well (see Fig. 5c). The re-dispatch of the power through the *ICs* mildly affects the operation of the DGs (see Fig. 4). On the other hand, since all the optimization is now active, the total operating cost of the MG decreases again [$C_T = 819.50$ ($/h$), see Fig. 5d].

Finally, the limits constraints for the power transfer through the *ICs* are activated at $t = 250s$. The power through the *IC* with the highest losses is decreased and those of the other two are increased (see Fig. 5a). The Lagrange multiplier associated with this constraint can be seen in Fig. 5b. Again, including the power transfer limits constraints slightly increases the total operating cost of the MG [$C_T = 819.52$ ($/h$), see Fig. 5d] and marginally affects the operation of the DGs (see Fig. 4).

TABLE IV
SUMMARY FOR THE TOTAL OPERATING COST.

Operating condition	Time	Cost ($/h)
Opt. within MGs	0s - 50s	820.55
Opt. among DGs	50s - 150s	819.55
$\boldsymbol{\lambda^{\mathrm{IC}}}$ consensus	150s - 250s	**819.50**
ICs limits constraint	250s - 400s	819.52

Summarizing, Table IV shows the operating cost for the HMG under all the studied scenarios. It can be seen that, as expected, the minimum operating cost is achieved when the full optimization is enabled (i.e., including λ^{IC} consensus). On the other hand, the total operating cost increases as new constraints are being incorporated in the controllers.

B. Test #2: Load-steps

Now, the performance of the proposed strategies against load steps is analyzed. The MG used in the previous test is simulated, maintaining the parameters and communication

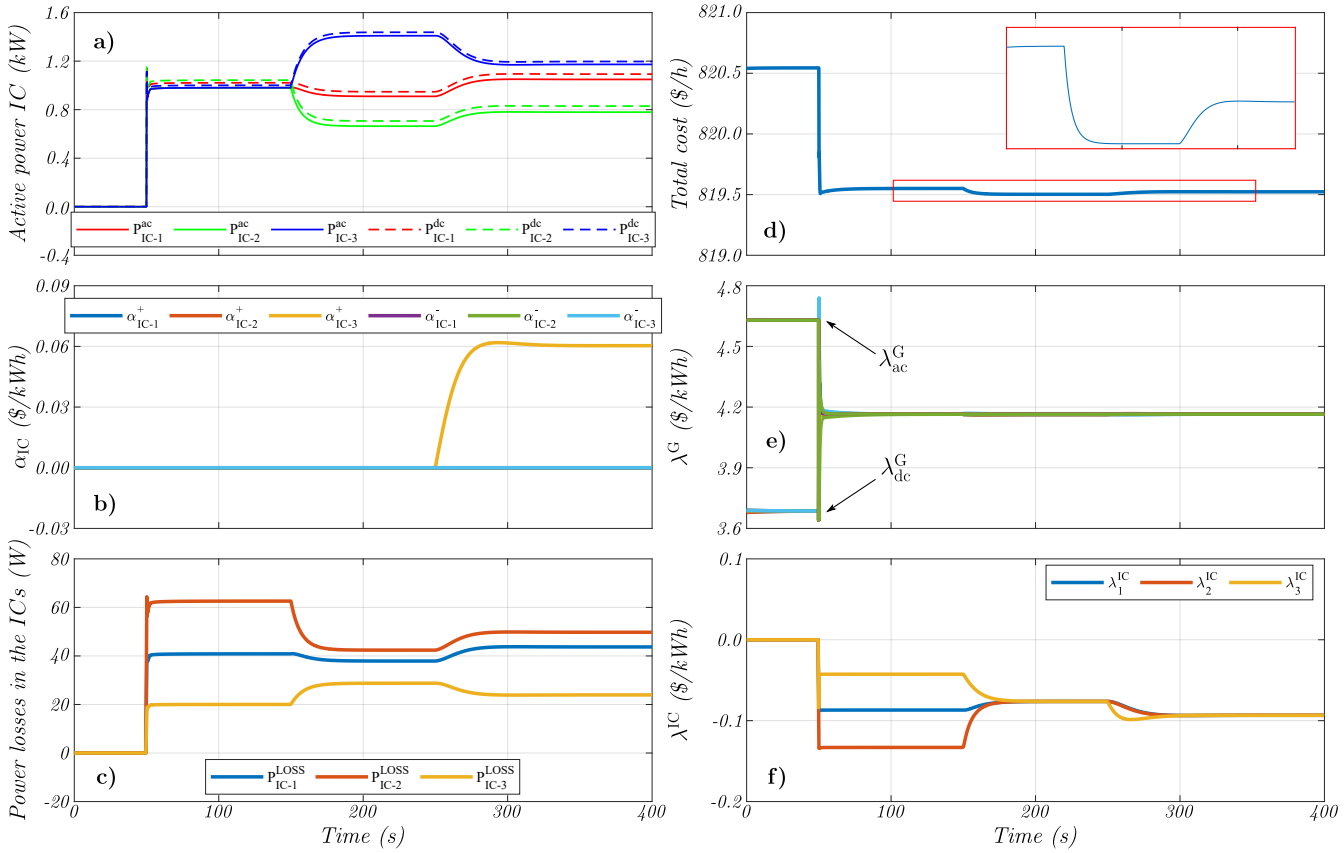

Fig. 5. Simulation Test #1: (a) Active power through the *ICs*. (b) Lagrange multiplier for transfer power constraints (α^{ac+}_{IC-k} and α^{ac-}_{IC-k}). (c) Power losses in the *ICs*. (d) Total operating cost. (e) Lagrange multiplier λ^G. (f) Lagrange multiplier λ^{IC}.

network (adjacency matrix) described before. The initial local-load of the 12 DGs is the same as in the previous test (see Table III). The results are shown in Fig. 6 and Fig. 7.

The simulation begins with all the controllers and the power limits constraints enabled, i.e., the full optimization of the MG is active. For $0s < t < 100s$, the DGs are achieving a λ^G consensus (see Fig. 7e) and the *ICs* are achieving λ^{IC} consensus (see Fig. 7f).

The total operating cost of the MG (see Fig. 7d) is minimum in this scenario [$C_T = 819.52$ ($/h$)], and the power through the IC_3 is touching the upper limit (see Fig. 7a for P^{dc}_{IC-3} and Fig. 7b for α^{+}_{IC-3}). On the other hand, the *dc*-DG$_1$ is generating its maximum power and the other DGs are operating within limits (see Fig. 6a for P^G_{ac-i}, Fig. 6d for P^G_{dc-j}, Fig. 6b for α^{+}_{ac-i}, and Fig. 6e for α^{+}_{dc-j}), while the secondary variables are regulated (see Fig. 6c for frequency and Fig. 6f for *dc*-voltage).

At $t = 100s$, a load step is applied at both sides of the HMG. The load at the *ac*-side is step-decreased to 13.7kW (76.1% of the nominal power at this side), while the load power at the *dc*-side is step-increased to 12.1kW (80.7% of the nominal power at this side). Due to the change in the load power, the power through the *ICs* decreases until it is negligible ($P^{ac}_{IC-k} \approx 0$), as shown in Fig. 7a. Moreover, the Lagrange multiplier associated with the power transfer limit (α^{+}_{IC-3}) slowly decreases until it becomes zero (see Fig. 7b). The only element that remains touching its upper operation limit is the *dc*-DG$_1$, which corresponds to the cheapest generator.

Despite the transient response, the secondary variables are maintained within limits all the time (see Fig. 6c for frequency and Fig. 6f for *dc*-voltage), and the λ consensuses are achieved by the DGs (see Fig. 7e for λ^G) and by the *ICs* (see Fig. 7f for λ^{IC}). The total operating cost for the new load condition is $C_T = 812.85$ ($/h$), as shown in Fig. 7d.

At $t = 200s$, a new load step is applied at both sides of the HMG; the load on the *ac*-side is step-decreased to 11.7kW (65.0% of the nominal power at this side), while the load power on the *dc*-side is step-increased to 13.1kW (87.3% of the nominal power at this side). Due to the change in the load, the power through the *ICs* now flows from the *ac*-MG to the *dc*-MG, as depicted in Fig. 7a. One more time, the *IC* with the lowest losses (IC_3) touches its operation limits and the Lagrange multiplier associated with this constraint is increased (see Fig. 7b for α^{-}_{IC-3}).

All DGs now are working within limits (see Fig. 6a for P^G_{ac-i}, and Fig. 6d for P^G_{dc-j}), which is reflected in the Lagrange multipliers associated with these constraints (see Fig. 6b for α^{+}_{ac-i}, and Fig. 6e for α^{+}_{dc-j}). On the other hand, all the secondary variables remain regulated within limits (see Fig. 6c for frequency and Fig. 6f for *dc*-voltage). One more time, the λ consensuses are achieved by the DGs (see Fig. 7e for λ^G) and by the *ICs* (see Fig. 7f for λ^{IC}) all the time, and the total operating cost for the new load condition is $C_T = 801.89$ ($/h$), as shown in Fig. 7d.

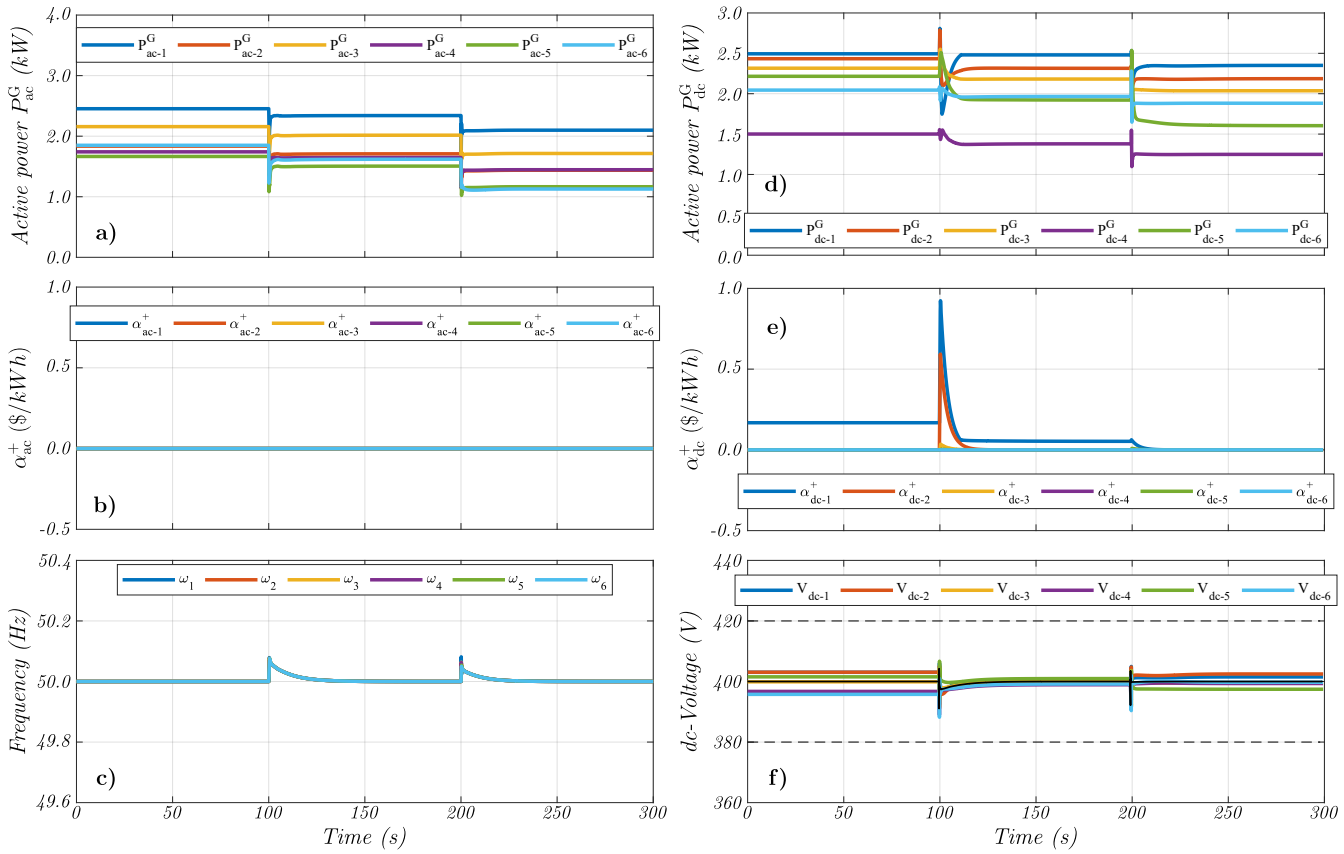

Fig. 6. Simulation Test #2: (a)&(d) Active power generated by *ac*-DGs ($P^{\mathrm{G}}_{\mathrm{ac}-i}$) and *dc*-DGs ($P^{\mathrm{G}}_{\mathrm{dc}-j}$). (b)&(e) Lagrange multiplier for generated power constraints ($\alpha^+_{\mathrm{ac}-i}$ and $\alpha^+_{\mathrm{dc}-j}$). (c)&(f) Secondary variables (frequency and *dc*-voltage).

VI. Conclusion

In this paper, a new consensus-based distributed secondary control strategy for HMGs has been proposed. This strategy considers the HMG as a single entity. The strategy is capable of restoring the variables modified by the primary control loop to their nominal values, while optimizing the dispatch of the DGs, in order to minimize the operation cost of the HMG. Additionally, when the HMG has multiple *ICs*, the power transfer is also dispatched between them towards total cost minimization.

The proposed strategy considers a reduced communication layer, as each agent in the HMG (i.e., each DG or *IC*) is communicating only with its neighbouring DGs and *ICs*. The proposed controller is capable of driving the MG to the optimal operation point while respecting the output limits of DGs and *ICs*. Simulation results were presented to validate the distributed consensus-based secondary control strategy for operating cost minimization (with multiple *ICs*) proposed in this paper. The validation through simulation was performed using a $33kW$ HMG with multiple *ICs*. The performance of the controllers in all the cases met the expectations.

References

[1] R. Lasseter, "Microgrids," in *2002 IEEE Power Engineering Society Winter Meeting. Conference Proceedings (Cat. No.02CH37309)*, vol. 1, 2002, pp. 305–308 vol.1.

[2] D. E. Olivares, A. Mehrizi-Sani, A. H. Etemadi, C. A. Cañizares, R. Iravani, M. Kazerani, A. H. Hajimiragha, O. Gomis-Bellmunt, M. Saeedifard, R. Palma-Behnke, G. A. Jiménez-Estévez, and N. D. Hatziargyriou, "Trends in microgrid control," *IEEE Trans. Smart Grid*, vol. 5, no. 4, pp. 1905–1919, 2014.

[3] N. Hatziargyriou, H. Asano, R. Iravani, and C. Marnay, "Microgrids," *IEEE Power and Energy Magazine*, vol. 5, no. 4, pp. 78–94, 2007.

[4] J. M. Guerrero, J. C. Vasquez, J. Matas, L. G. de Vicuna, and M. Castilla, "Hierarchical control of droop-controlled ac and dc microgrids—a general approach toward standardization," *IEEE Trans. Ind. Electron.*, vol. 58, no. 1, pp. 158–172, 2011.

[5] T. Dragičević, X. Lu, J. C. Vasquez, and J. M. Guerrero, "DC Microgrids—Part I: A Review of Control Strategies and Stabilization Techniques," *IEEE Trans. Power Electron.*, vol. 31, no. 7, pp. 4876–4891, July 2016.

[6] Y. Khayat, Q. Shafiee, R. Heydari, M. Naderi, T. Dragičević, J. W. Simpson-Porco, F. Dörfler, M. Fathi, F. Blaabjerg, J. M. Guerrero, and H. Bevrani, "On the secondary control architectures of ac microgrids: An overview," *IEEE Trans. Power Electron.*, vol. 35, no. 6, pp. 6482–6500, 2020.

[7] T. Dragičević, X. Lu, J. C. Vasquez, and J. M. Guerrero, "Dc microgrids—part ii: A review of power architectures, applications, and standardization issues," *IEEE Trans. Power Electron.*, vol. 31, no. 5, pp. 3528–3549, 2016.

[8] S. K. Sahoo, A. K. Sinha, and N. K. Kishore, "Control techniques in ac, dc, and hybrid ac–dc microgrid: A review," *IEEE Trans. Emerg. Sel. Topics Power Electron.*, vol. 6, no. 2, pp. 738–759, 2018.

[9] A. Hirsch, Y. Parag, and J. Guerrero, "Microgrids: A review of technologies, key drivers, and outstanding issues," *Renewable and Sustainable Energy Reviews*, vol. 90, pp. 402 – 411, 2018. [Online]. Available: http://www.sciencedirect.com/science/article/pii/S136403211830128X

[10] A. A. Jabbar, A. Y. Elrayyah, M. Z. Wanik, A. P. Sanfilippo, and N. K. Singh, "Development of Hybrid AC/DC Laboratory-scale Smart Microgrid Testbed with Control Monitoring System Implementation in LabVIEW," in *2019 IEEE PES GTD Gd. Int. Conf. Expo. Asia, GTD*

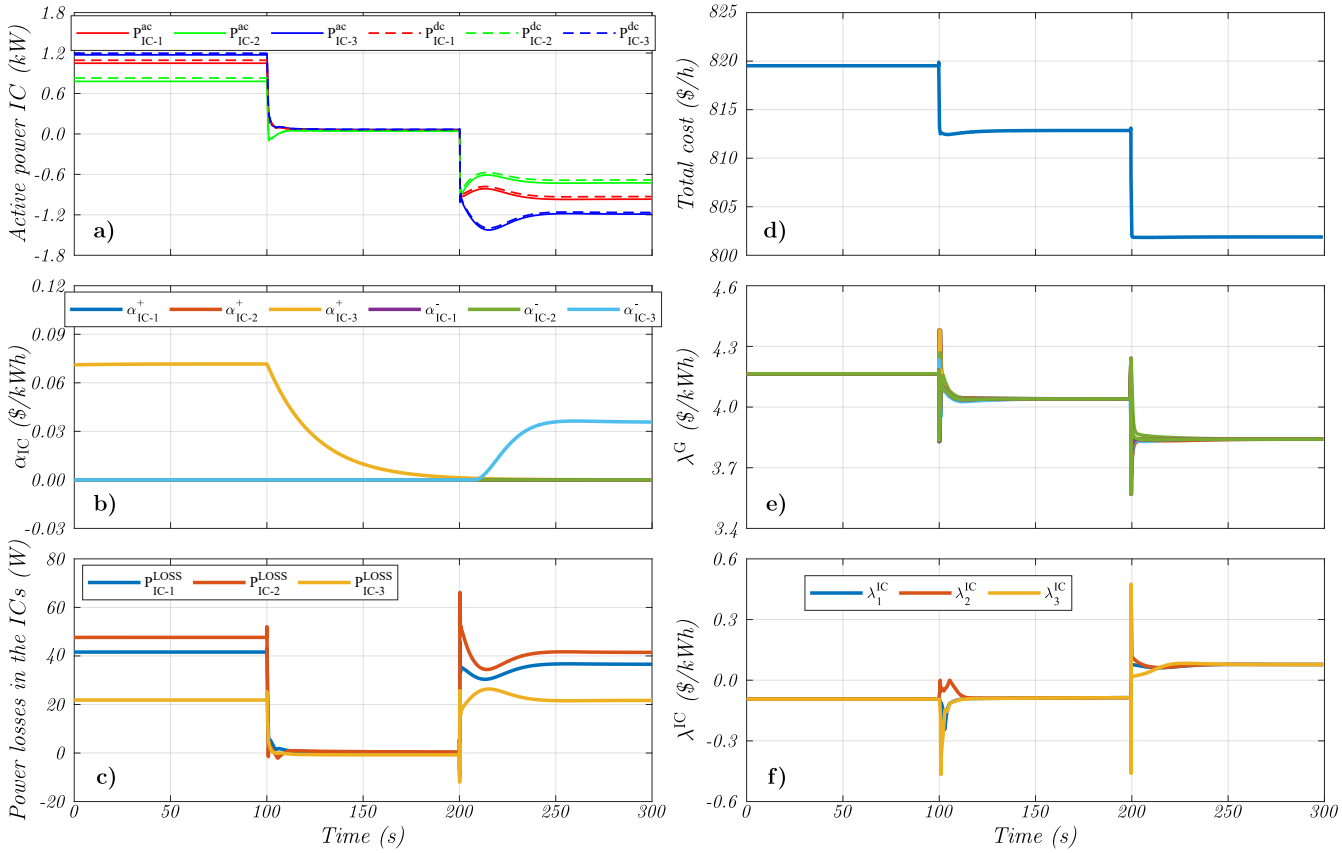

Fig. 7. Simulation Test #2: (a) Active power through the *ICs*. (b) Lagrange multiplier for transfer power constraints ($\alpha^{\mathrm{ac}+}_{\mathrm{IC}-k}$ and $\alpha^{\mathrm{ac}-}_{\mathrm{IC}-k}$). (c) Power losses in the *ICs*. (d) Total operating cost. (e) Lagrange multiplier λ^{G}. (f) Lagrange multiplier λ^{IC}.

Asia 2019, may 2019, pp. 889–894.

[11] P. C. Loh, D. Li, Y. K. Chai, and F. Blaabjerg, "Autonomous Control of Interlinking Converter With Energy Storage in Hybrid AC-DC Microgrid," *IEEE Trans. Ind. Appl.*, vol. 49, no. 3, pp. 1374–1382, May 2013.

[12] E. Espina, J. Llanos, C. Burgos-Mellado, R. Cárdenas-Dobson, M. Martínez-Gómez, and D. Sáez, "Distributed control strategies for microgrids: An overview," *IEEE Access*, vol. 8, pp. 193 412–193 448, 2020.

[13] Q. Zhou, M. Shahidehpour, A. Paaso, S. Bahramirad, A. Alabdulwahab, and A. Abusorrah, "Distributed control and communication strategies in networked microgrids," *IEEE Communications Surveys Tutorials*, vol. 22, no. 4, pp. 2586–2633, 2020.

[14] P. C. Loh, D. Li, Y. K. Chai, and F. Blaabjerg, "Autonomous operation of hybrid microgrid with ac and dc subgrids," *IEEE Trans. Power Electron.*, vol. 28, no. 5, pp. 2214–2223, 2013.

[15] P. Wang, C. Jin, D. Zhu, Y. Tang, P. C. Loh, and F. H. Choo, "Distributed control for autonomous operation of a three-port ac/dc/ds hybrid microgrid," *IEEE Trans. Ind. Electron.*, vol. 62, no. 2, pp. 1279–1290, 2015.

[16] P. C. Loh, D. Li, Y. K. Chai, and F. Blaabjerg, "Hybrid ac–dc microgrids with energy storages and progressive energy flow tuning," *IEEE Trans. Power Electron.*, vol. 28, no. 4, pp. 1533–1543, 2013.

[17] Y. Cao, X. Pan, and Y. Sun, "Dynamic economic dispatch of ac/dc hybrid microgrid based on consensus algorithm," in *2019 IEEE 3rd Conf. on Energy Internet and Energy Syst. Integr. (EI2)*, 2019, pp. 319–324.

[18] L. Li, X. Bai, Y. Guo, J. Zhang, C. Chen, Y. Yi, and A. Wang, "Distributed optimal dispatching of ac/dc hybrid microgrid based on consensus algorithm," in *2021 6th Asia Conference on Power and Electrical Engineering (ACPEE)*, 2021, pp. 1398–1402.

[19] B. Papari, G. Ozkan, H. P. Hoang, P. R. Badr, C. S. Edrington, H. Parvaneh, and R. Cox, "Distributed control in hybrid ac-dc microgrids based on a hybrid mcsa-admm algorithm," *IEEE Open J. of Ind. Appl.*, vol. 2, pp. 121–130, 2021.

[20] Q. Zhou, M. Shahidehpour, Z. Li, and X. Xu, "Two-layer control scheme for maintaining the frequency and the optimal economic operation of hybrid ac/dc microgrids," *IEEE Trans. Power Syst.*, vol. 34, no. 1, pp. 64–75, 2019.

[21] Q. Zhou, M. Shahidehpour, Z. Li, L. Che, A. Alabdulwahab, and A. Abusorrah, "Compartmentalization strategy for the optimal economic operation of a hybrid ac/dc microgrid," *IEEE Trans. Power Syst.*, vol. 35, no. 2, pp. 1294–1304, 2020.

[22] P. Lin, C. Jin, J. Xiao, X. Li, D. Shi, Y. Tang, and P. Wang, "A distributed control architecture for global system economic operation in autonomous hybrid ac/dc microgrids," *IEEE Trans. Smart Grid*, vol. 10, no. 3, pp. 2603–2617, 2019.

[23] N. Ahmad Khan, "Power loss modeling of isolated ac/dc converter," Master's thesis, KTH, Electrical Energy Conversion, 2012.

[24] J. W. Simpson-Porco, Q. Shafiee, F. Dörfler, J. C. Vásquez, J. M. Guerrero, and F. Bullo, "Secondary Frequency and Voltage Control of Islanded Microgrids via Distributed Averaging," *IEEE Trans. Ind. Electron.*, vol. 62, no. 11, pp. 7025–7038, Nov 2015.

[25] E. Espina, R. Cárdenas-Dobson, J. W. Simpson-Porco, D. Sáez, and M. Kazerani, "A consensus-based secondary control strategy for hybrid ac/dc microgrids with experimental validation," *IEEE Trans. Power Electron.*, vol. 36, no. 5, pp. 5971–5984, 2021.

[26] Q. Shafiee, V. Nasirian, J. C. Vasquez, J. M. Guerrero, and A. Davoudi, "A multi-functional fully distributed control framework for ac microgrids," *IEEE Trans. Smart Grid*, vol. 9, no. 4, pp. 3247–3258, 2018.

[27] Z. Li, Z. Duan, G. Chen, and L. Huang, "Consensus of multiagent systems and synchronization of complex networks: A unified viewpoint," *IEEE Trans. Circuits Syst. I, Reg. Papers*, vol. 57, no. 1, pp. 213–224, 2010.

[28] D. Spanos, R. Olfati-saber, and R. Murray, "Dynamic consensus on mobile networks," *Proc. 16th Int. Fed. Autom. Control, Prague, Czech Republic*, 01 2005.

[29] E. Espina *et al.*, "Appendix A: Hybrid *ac/dc*-Microgrid Topology." web address: http://www.e2tech.cl/wp-content/uploads/2022/04/Systemdescription.pdf, 2022.